Supporting Information for

Original article

Targeted inhibition of Gus-expressing *Enterococcus faecalis* to promote intestinal stem cell and epithelial renovation contributes to the relief of irinotecan chemotoxicity by dehydrodiisoeugenol

Ruiyang Gao[a,†], Bei Yue[a,†], Cheng Lv[b], Xiaolong Geng[a], Zhilun Yu[a], Hao Wang[a], Beibei Zhang[a], Fangbin Ai[a], Ziyi Wang[a], Donghui Liu[a], Zhengtao Wang[a,*], Kaixian Chen[a,c,*], Wei Dou[a,*]

[a]*The MOE Key Laboratory of Standardization of Chinese Medicines, Shanghai Key Laboratory of Compound Chinese Medicines, and the SATCM Key Laboratory of New Resources and Quality Evaluation of Chinese Medicines, Institute of Chinese Materia Medica, Shanghai University of Traditional Chinese Medicine, Shanghai 201203, China*

[b]*Centre for Chinese Herbal Medicine Drug Development Limited, Hong Kong Baptist University, Hong Kong SAR 999077, China*

[c]*Shanghai Institute of Materia Medica, Chinese Academy of Sciences, Shanghai 201210, China*

Received 26 March 2024; received in revised form 25 June 2024; accepted 26 July 2024

*Corresponding authors:

E-mail addresses: ztwang@shutcm.edu.cn (Zhengtao Wang), kxchen@simm.ac.cn (Kaixian Chen), douwei@shutcm.edu.cn (Wei Dou).

[†]These authors made equal contributions to the work.

Supplementary materials include:

Table S1. The list of primers used for reverse transcription quantitative polymerase chain reaction (RT-qPCR)

Table S2. Taxa composition of dominant bacteria (abundance ≥ 0.01%) at phylum and the major *β*-glucuronidase (Gus)-producing bacteria at genus

Supplementary methods

Supplementary figure legends

Table S1. The list of primers used for RT-qPCR.

Gene	Forward primer (5′–3′)	Reverse primer (5′–3′)
Cyclooxygenase-2 (*Cox-2*)	GCCTTCCCTACTTCACAA	ACAACTCTTTTCTCATTTCCAC
Interleukin (*Il*)*-6*	GGCGGATCGGATGTTGTGAT	GGACCCCAGACAATCGGTTG
Tumor necrosis factor (*Tnf*)*-α*	CTCTTCTCATTCCTGCTTGT	GTGGTTTGTGAGTGTGAGG
Zonula occludens (*Zo*)*-1*	GCCGCTAAGAGCACAGCAA	TCCCCACTCTGAAAATGAGGA
Claudin-7	GGCCACTCGAGCCTTAATGGTG	CCTGCCCAGCCGATAAAGATGG
Occludin	ATGTCCGGCCGATGCTCTC	TTTGCTGCTCTTGGGTCTGTAT
Leucine-rich repeat-containing G-protein-coupled receptor 5 (*Lgr5*)	CCTACTCGAAGACTTACCCAGT	GCATTGGGGTGAATGATAGCA
Polycomb ring finger (*Bmi1*)	CCCCACTTAATGTGTGTCCTG	TTGCTGGTCTCCAAGTAACG
Achaete-scute family bHLH transcription factor 2 (*Ascl2*)	AGGACGCAATAAGCTAAGCATC	AGTGGACGTTTGCACCTTCACG
β-Defensin1	GGCTGCCACCACTATGAAAACTC	GAGACAGAATCCTCCATGTTGAA
β-Defensin2	CTCCACCTGCAGCTTTTAGC	GCTAGGGAGCACTTGTTTGC
Lysozyme 1 (*Lyz1*)	GAGACCGAAGCACCGACTATG	CGGTTTTGACATTGTGTTCGC
Krüppel-like transcription factors 4 (*Klf4*)	AGGAACTCTCTCACATGAAGCG	GGTCGTTGAACTCCTCGGTC
Protease-resistant trefoil factor 3 (*Tff3*)	CAGATTACGTTGGCCTGTCTCC	ATGCTTGCTACCCTTGGACCAC
Mucin 2 (*Muc2*)	TGCCCACCTCCTCAAAGAC	TAGTTTCCGTTGGAACAGTGAA
Doublecortin-like kinase 1 (*Dclk1*)	TGAACAAGAAGACGGCTCACTCC	GCTGGTGGGTGATGGACTTGG
Transient receptor potential channel subfamily M member 5 (*Trpm5*)	CCTCCGTGCTTTTTGAACTCC	CATAGCCAAAGGTCGTTCCTC
β-Actin	GGGAAATCGTGCGTGAC	AGGCTGGAAAAGAGCCT
g_Enterococcus	ATCAGAGGGGGATAACACTT	ACTCTCATCCTTGTTCTTCTC
g_Bacteroides	GAGAGGAAGGTCCCCCAC	CGCTACTTGGCTGGTTCAG
g_Parabacteroides	GCGTTCCATTAGGCAGTTG	AGGAGTTTGGTCCGTGTCTC
g_Lactobacillus	TGGAAACAGRTGCTAATACCG	GTCCATTGTGGAAGATTCCC
Enterococcus faecalis (*E. faecalis*)	ACCAATGTTGGCACAAGAAA	TTTCGTTCAAGCGGTCTTTT
Enterococcus faecium (*E. faecium*)	ACGGAGATCGTGGATTCAAA	CGTACGGGAAGTGATTCGAC
All bacteria	CGGTGAATACGTTCCCGG	TACGGCTACCTTGTTACGACTT

Table S2. Taxa composition of dominant bacteria (abundance ≥ 0.01%) at phylum and the major Gus-producing bacteria at genus.

Taxonomy	Control (Mean±SEM)	CPT11 (Mean±SEM)	CPT11+DDIE (Mean±SEM)	*p*-value (CPT11 *vs*. Con)	*p*-value (CPT11+DDIE *vs*. DDIE)
Bacteroidota	0.4344±0.0995	0.3474±0.0751	0.3626±0.0438	0.5073	0.8685
Firmicutes	0.4542±0.0856	0.4290±0.0839	0.4023±0.0404	0.8381	0.7802
Proteobacteria	0.0347±0.0342	0.0545±0.0253	0.0644±0.0295	0.6523	0.8045
Verrucomicrobiota	0.0002±0.0002	0.0424±0.0179	0.0479±0.0356	0.0401	0.8923
Actinobacteriota	0.0248±0.0228	0.0386±0.0189	0.0253±0.0116	0.6784	0.6154
Campilobacteriota	0.0152±0.0043	0.0332±0.0083	0.0564±0.0233	0.0828	0.3703
Chloroflexi	0.0037±0.0037	0.0062±0.0037	0.0039±0.0022	0.6406	0.5971
Deferribacterota	0.0011±0.0004	0.0056±0.0023	0.0100±0.0085	0.0779	0.6274
Desufobacterota	0.0092±0.0021	0.0146±0.0031	0.0102±0.0021	0.1836	0.2656
Gemmatimonadota	0.0023±0.0023	0.0036±0.0021	0.0022±0.0013	0.6759	0.5984
Bdellovibrionota	0.0030±0.0030	0.0046±0.0027	0.0029±0.0016	0.7005	0.5885
Nitrospirota	0.0018±0.0018	0.0026±0.0016	0.0014±0.0008	0.723	0.5264
Patescibacteria	0.0068±0.0019	0.0048±0.0017	0.0024±0.0011	0.4599	0.257
Alistipes	0.0398±0.0085	0.0072±0.0025	0.0142±0.0038	0.0103	0.1734
Bacteroides	0.0566±0.0112	0.1226±0.0809	0.0472±0.0100	0.4493	0.3905
Parabacteroides	0.0057±0.0015	0.0126±0.0023	0.0064±0.0011	0.0509	0.0527
Prevotella	0.0000±0.0016	0.0011±0.0007	0.0000±0.0000	0.1421	0.1567
Anaerotruncus	0.0012±0.0000	0.0072±0.0025	0.0026±0.0007	0.0509	0.1229
Blautia	0.0009±0.0004	0.0018±0.0002	0.0021±0.0006	0.1158	0.6450
Enterococcus	0.0000±0.0000	0.0008±0.0002	0.0001±0.0000	0.0057	0.0077
Lactobacillus	0.0540±0.0332	0.2462±0.1559	0.1394±0.0123	0.1551	0.3231
Roseburia	0.0145±0.0048	0.0038±0.0014	0.1015±0.0019	0.0774	0.0376

1. Supplementary methods

1.1. Cell viability assay

NCM460 normal human intestinal epithelial cells and CT26 murine colon carcinoma cells were seeded into 96-well plates and incubated with various concentrations of DDIE and/or SN38. Following a 24 h treatment, the original culture medium was replaced with culture medium containing 10% Cell Counting Kit-8 (CCK-8; Dojindo, Kumamato, Japan) reagent. The cells were then incubated in the dark at 37 °C for 30 min, and the optical density (OD) was measured at 450 nm using a microplate reader. Relative cell viability (%) = [OD (treated) – OD (blank)] / [OD (control) – OD (blank)] × 100.

1.2. Transepithelial electrical resistance (TEER) assay

NCM460 cells (5×10^4 cells/400 μL/well) were seeded in 24-well plates containing Millicell culture inserts, with 600 μL of Roswell Park Memorial Institute-1640 basal medium added externally to the inserts. The medium was replaced every other day, and the TEER of the monolayer was measured using an MERS00002 ohmmeter. When the resistance reached 200 $\Omega\cdot cm^2$, indicating the formation of a tight cell monolayer, drug administration was initiated with SN38 (250 nmol/L), DDIE (15 μmol/L), or a combination of SN38 (250 nmol/L) + DDIE (15 μmol/L), followed by continued incubation. TEER values were measured at 0, 12, 24, 48, and 96 h after administration.

1.3. Scratch healing assay

The migration of NCM460 cells was assessed using the ibidi insert-based scratch assay. NCM460 cells were seeded into the inserts at a concentration of 5×10^4 cells/mL, with 70 μL per chamber. Once the cells reached confluence in the insert area, the inserts were carefully removed. Cells were treated with serum-free medium containing 15 μmol/L DDIE, 500 nmol/L SN38, or a combination of SN38 (500 nmol/L) and DDIE (15 μmol/L). Images of the scratch area were captured using an inverted microscope at 0 and 24 h after drug treatment. The width of the scratch area was measured using ImageJ software. Relative migration distance (%) = [width (0 h, treated) - width (24 h, treated)] / [width (0 h, control) - width (24 h, control)] × 100.

1.4. Flow cytometry

NCM460 cells were seeded, treated with DDIE (15 μmol/L), SN38 (500 nmol/L), or a combination for 24 h. The culture medium was aspirated, cells were digested with trypsin without ethylene diamine tetraacetic acid, centrifuged at 300 × *g* for 5 min, washed twice with pre-chilled PBS, and then resuspended in 1× Binding Buffer to achieve a cell density of 3×10^6 cells/mL. 100 μL of cell suspension was mixed with 5 μL of Annexin V-FITC and incubated in the dark at room temperature for 15 min. Before flow cytometry analysis, 5 μL of PI dye was added, followed by the addition of 300 μL of 1× Binding Buffer for thorough mixing. Flow cytometry (Beckman Coulter, Brea, USA) was performed, and Guava flow cytometry software was used for analysis.

1.5. Molecular docking simulation

Three dimensional (3D) structure of Gus protein (PDB: 3K46) was obtained from the RCSB PDB database (https://www.rcsb.org/structure/3K46). The initial structure of the protein was pre-processed using Autodock Tools version 4.2.6 by removing water molecules and adding hydrogen atoms and exported to the pdbqt file for docking. Obtain the 2D structures of the Gus inhibitor (PubChem SID: 482821795) and DDIE (PubChem SID: 5379033) from the PubChem database and convert it into a Mol2 file using OpenBabel software. The DDIE structure was used for subsequent analysis by adding hydrogen atoms, self-distributing charge, and torsional construction detection. The coordinates of the central grid point of maps were (25.201, –3.939, 43.523), and the number of grid points in the XYZ of grid box was 126 × 120 × 126. The docking was performed by using Autodock Tools, and the docking results were optimized by using PyMOL Molecular Graphics System software.

1.6. Gus enzyme activity assay in vitro

The inhibiting ability of DDIE on *E.coli* Gus (Sigma–Aldrich, USA) was assessed by using a fluorescent substrate 4-MUG. The standard reaction buffer contained 75 mmol/L phosphate buffer (pH = 6.8), 40 μL of 500 ng/mL Gus, 30 μL of 500 μmol/L 4-MUG, and various concentrations of DDIE (0, 40, 60, 80, 100, 200 μmol/L). The reaction was carried out in a final volume of 100 μL. After incubating for 30 min, the fluorescence intensities were measured using a microplate reader at a wavelength of 405 nm.

1.7. Mice gut microbiota clearance experiment

Male BALB/c mice (6 weeks old, weighing 20–22 g) were subjected to a consecutive three-day regimen of oral administration, with each animal receiving 200 μL of an antibiotic combination solution (composed of 1 g/L ampicillin, 1 g/L metronidazole, 0.5 g/L neomycin sulfate, and 0.5 g/L vancomycin) to effectively eliminate their intestinal microbiota. Subsequently, the drinking water for the mice was replaced with the antibiotic mixture, provided for free access. The mice were then randomly divided into two groups: the CPT11-ABX group (CPT11 = 60 mg/kg, *n* = 6) and the CPT11+DDIE-ABX group (CPT11 = 60 mg/kg, DDIE = 75 mg/kg, *n* = 6). Starting from Day 3, DDIE was delivered daily *via* oral gavage in a volume of 200 μL until the 13-day study conclusion. Both groups received intraperitoneal injection of CPT11 to induce modeling from Days 5 to 9.

Supporting Figures

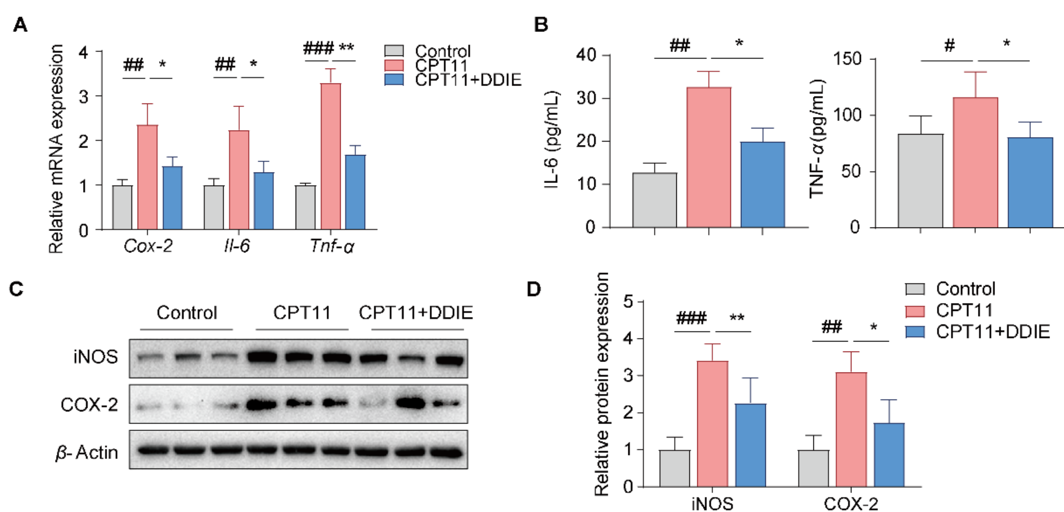

Figure S1. DDIE inhibited pro-inflammatory mediators in CPT11-induced mucositis mice. (A) The relative mRNA levels of the *Cox-2*, *Il-6*, *Tnf-α* in colon tissues across each group (n = 6). (B) Serum concentrations of IL-6 and TNF-α in mice (n = 6). (C, D) Representative western blots and quantitative analysis of iNOS and COX-2 in colon tissues (n = 3). Data are expressed as mean ± SD. $^{\#}P < 0.05$, $^{\#\#}P < 0.01$ and $^{\#\#\#}P < 0.001$ *vs*. Control group; $^{*}P < 0.05$, $^{**}P < 0.01$ *vs*. CPT11 group.

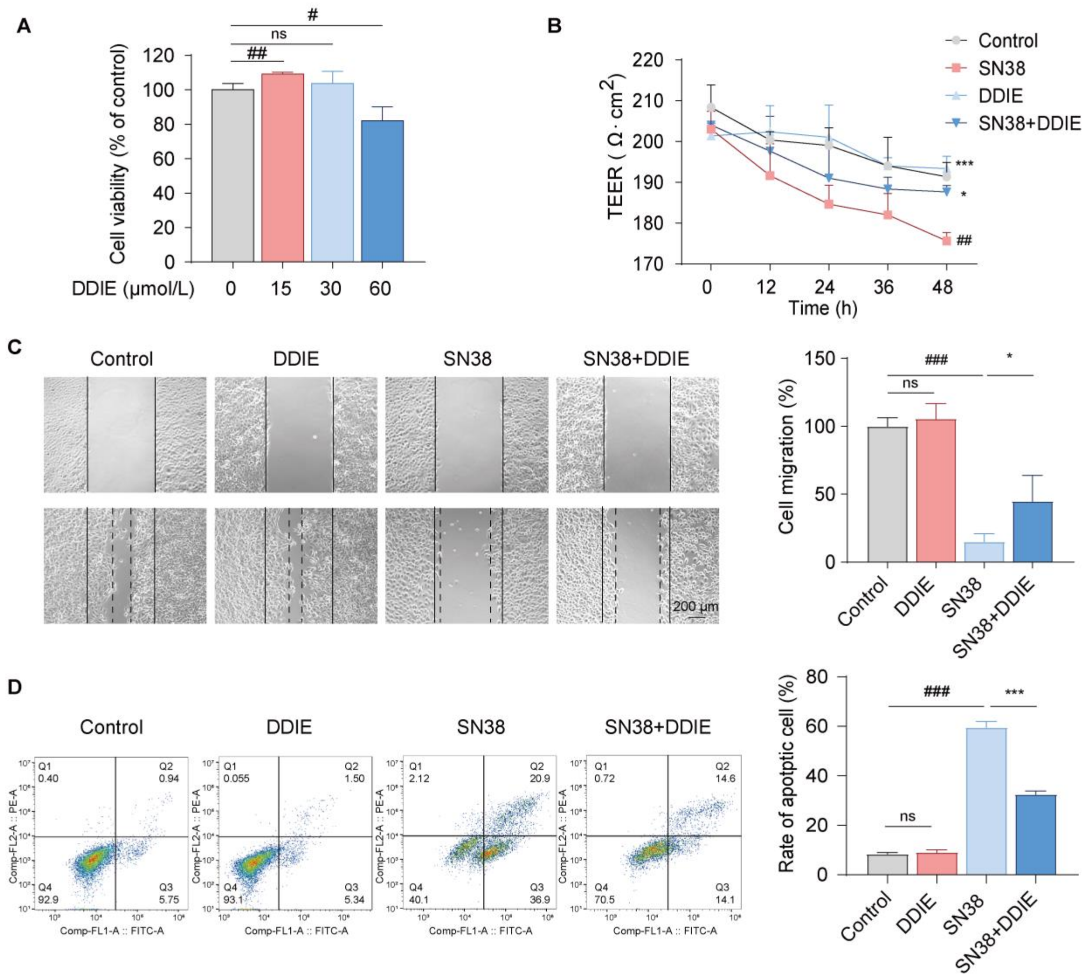

Figure S2. DDIE enhanced the integrity of the epithelial barrier and facilitated the repair of NCM460 human normal intestinal epithelial cells. (A) Effect of DDIE on NCM460 cell viability. Cells were treated with DDIE (15, 30, 60 μmol/L) for 24 h, and then cell viability was measured (*n* = 3). (B) NCM460 cell monolayers were treated with DDIE (15 μmol/L), SN38 (250 nmol/L), or SN38 (250 nmol/L) + DDIE (15 μmol/L) for 12, 24, 36, and 48 h, respectively; then, we measured TEER (*n* = 3). (C) Representative images of scratch wound assays for NCM460 cell monolayers at 0 and 24 h after scratching (*n* = 3). (D) Effect of DDIE on cell apoptosis induced by SN38 was detected by flow cytometry (*n* = 3). Data are expressed as mean ± SD. $^{\#}P < 0.05$, $^{\#\#}P < 0.01$, and $^{\#\#\#}P < 0.001$ *vs*. Control group; $^{*}P < 0.05$, $^{***}P < 0.001$ *vs*. SN38 group. ns, not significant.

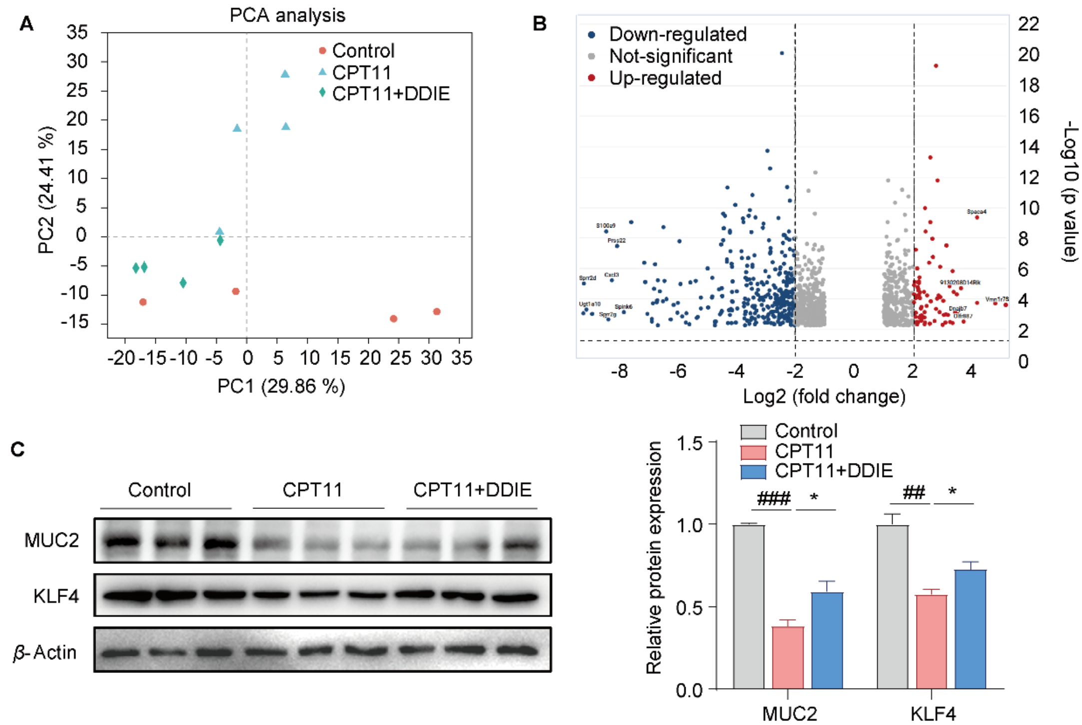

Figure S3. DDIE modulated the overall gene expression profile and goblet cell differentiation-associated genes in CPT11-induced mucositis mice. (A) Principal component analysis (PCA) plot of colon RNA-seq data in the group of Control (round red dot), CPT11 (triangular blue dot) and CPT11+DDIE (rhomboid green dot) ($n = 4$). (B) Volcano plot of differentially genes in colon of CPT11+DDIE group *vs*. CPT11 group identified using DESeq2 analysis. Blue dots represented down-regulated genes (CPT11+DDIE vs CPT11 folds change of < –2), red dots meant up-regulated genes (CPT11+DDIE vs CPT11 folds change of > 2), and gray dots showed genes with no statistically significant difference ($n = 4$). (C) Representative western blots and quantitative analysis of MUC2 and KLF4 in colon tissues ($n = 3$). Data are represented as mean ± SD. $^{###}P < 0.001$ *vs*. Control group, $^{*}P < 0.05$ *vs*. CPT11 group.

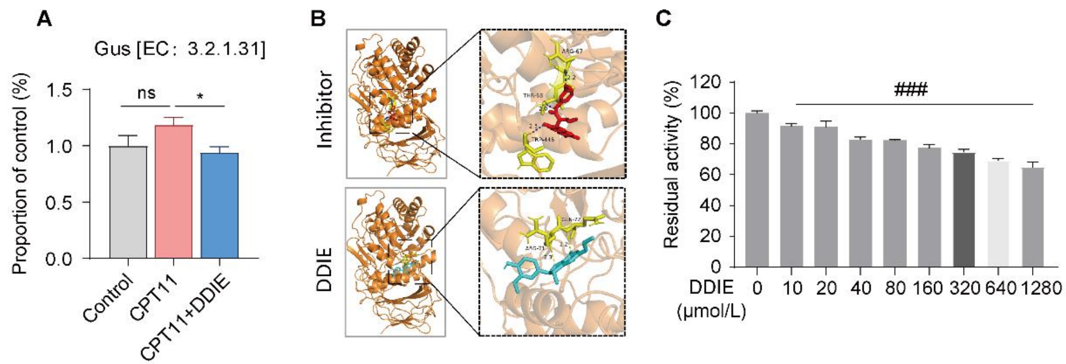

Figure S4. DDIE suppressed the activity of Gus enzyme. (A) Proportional abundance of ortholog K01195 (KO: K01195; description: beta-glucuronidase [EC: 3.2.1.31]) according to the Kyoto Encyclopedia of Genes and Genomes database (n = 4). (B) A stereo view of the binding model of *Escherichia coli* Gus (PDB: 3K46) combined with inhibitor or DDIE. (C) Effects of DDIE (0, 10, 20, 40, 80, 160, 320, 640, 1280 μmol/L) on the residual activity of Gus derived from *E. coli* by *in vitro* antibacterial experiment (n = 3). Data are expressed as mean ± SD (n = 3). $^{###}P < 0.001$ *vs*. Control group, $^{*}P < 0.05$ *vs*. CPT11 group. ns, not significant.

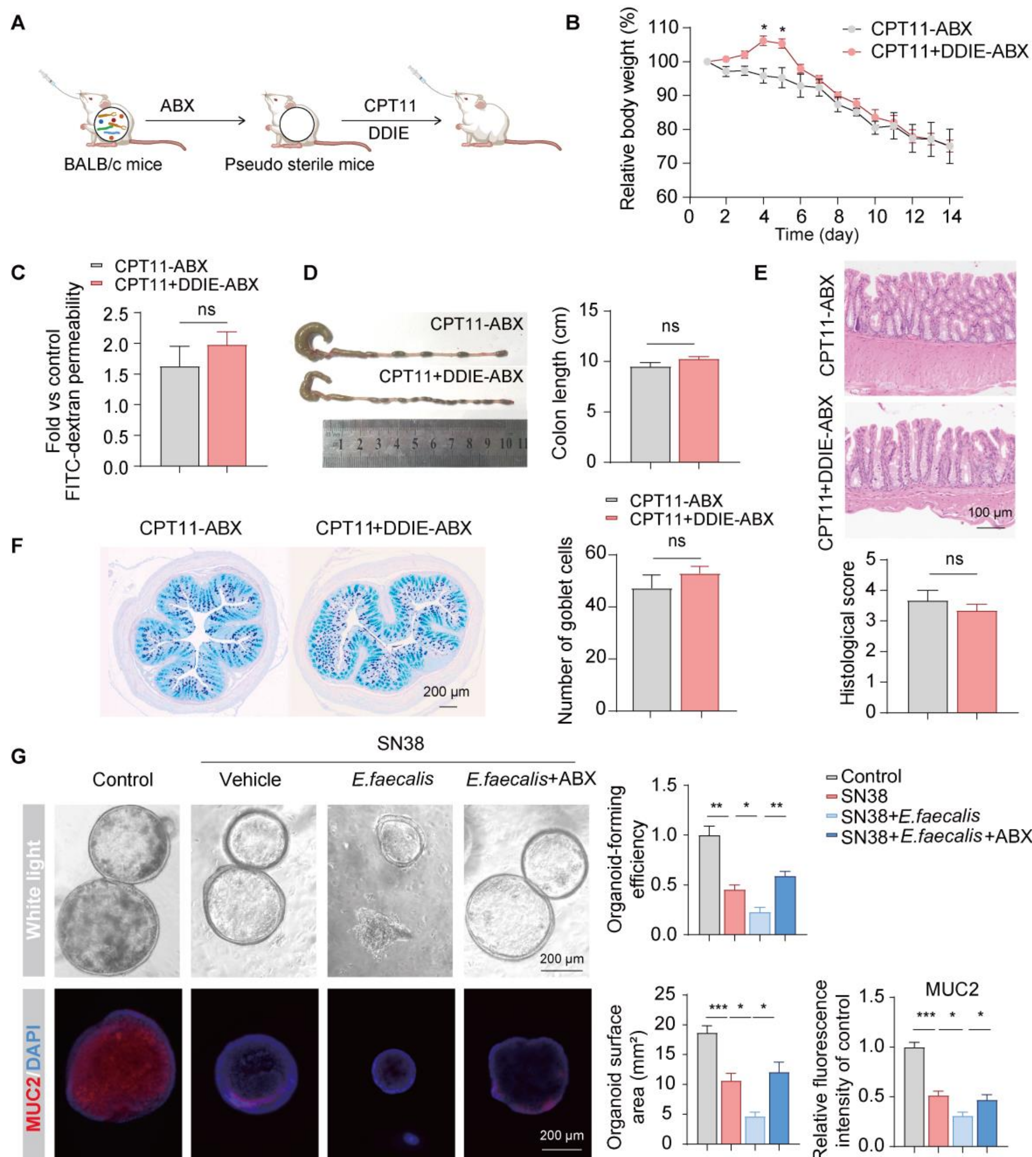

Figure S5. Antibiotics treatment abolished the beneficial effect of DDIE on CPT11-induced mice mucositis. (A) Schematic diagram of the experimental procedure. (B) Body weight was recorded following the animal experiment. Data were plotted as a percentage of basal body weight. Data are expressed as mean ± SEM (*n* = 6-8). (C) Serum concentrations of FITC-dextran in mice (*n* = 4–5). (D) The representative colon was photographed and colon length was measured (*n* = 6). (E) The representative colon H&E staining and histological scores analysis (*n* = 6). (F) Representative AB-PAS staining of the colonic sections and the counting of goblet cells per villus calculation unit (*n* = 3). (G) The colonic organoids were treated with SN38 (100 nmol/L), SN38 (100 nmol/L) + *E. faecalis* (10^6 CFU), or SN38 (100 nmol/L) + *E. faecalis* (10^6 CFU) + ABX for 24 h on day 2 of culture. Samples were visualized under a fluorescence microscope. Representative bright-field and

immunofluorescence images (MUC2: red; DAPI: blue) of organoids are shown (left panel). Qualitative statistics of the organoid surface area, the rate of organoid formation, and the MUC2 fluorescence intensity of the organoids (right panel). Data are expressed as mean ± SD. $^{*}P < 0.05$, $^{**}P < 0.01$, and $^{***}P < 0.001$. ns, not significant.

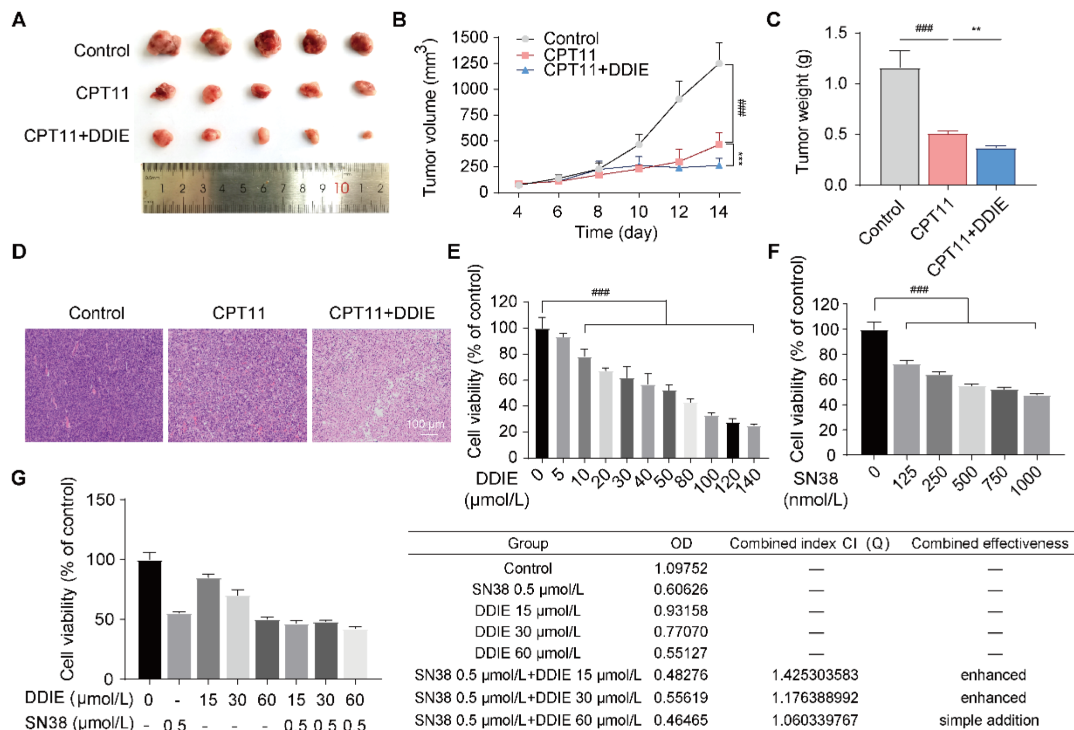

Group	OD	Combined index CI (Q)	Combined effectiveness
Control	1.09752	—	—
SN38 0.5 μmol/L	0.60626	—	—
DDIE 15 μmol/L	0.93158	—	—
DDIE 30 μmol/L	0.77070	—	—
DDIE 60 μmol/L	0.55127	—	—
SN38 0.5 μmol/L+DDIE 15 μmol/L	0.48276	1.425303583	enhanced
SN38 0.5 μmol/L+DDIE 30 μmol/L	0.55619	1.176388992	enhanced
SN38 0.5 μmol/L+DDIE 60 μmol/L	0.46465	1.060339767	simple addition

Figure S6. DDIE synergistically enhanced the anti-tumor effects of CPT11 in a colon cancer xenograft model. (A) Representative gross images of the tumor (n = 5). (B) The volume of tumors in mice during a 2-week administration of CPT11, or CPT11+DDIE (n = 6). (C) The weight of tumors in mice with the intervention of CPT11, or CPT11+DDIE (n = 6). (D) Representative images of H&E staining of tumor tissues. (E, F) The cytotoxic effects of SN38 or DDIE on CT26 mouse colorectal cancer cells (n = 3). (G) The cytotoxic effects of SN38 alone or combined with DDIE on CT26 mouse colorectal cancer cells, and the calculation of combined index (n = 3). Data are expressed as mean ± SD. $^{###}P < 0.001$ *vs*. Control group, $^{**}P < 0.01$, $^{***}P < 0.001$ *vs*. CPT11 group.